Available online at www.sciencedirect.com
ScienceDirect
Journal of Sound and Vibration 319 (2009) 1136–1149
JOURNAL OF SOUND AND VIBRATION
www.elsevier.com/locate/jsvi

Comments on nonlinear dynamics of a non-ideal Duffing-Rayleigh oscillator: Numerical and analytical approaches

Jorge L. Palacios Felix, José M. Balthazar*, R.M.L.R.F. Brasil[1]

UNESP-Rio Claro, Department of Statistics, Applied Mathematics and Computation (DEMAC), Av. 24A, Bela Vista 1515, 13506-700 Rio Claro, Brazil

Received 23 June 2007; received in revised form 18 May 2008; accepted 20 June 2008
Handling Editor: S. Bolton
Available online 8 August 2008

Abstract

An analytical and numerical investigation into the dynamic interaction between a cantilever beam with nonlinear damping and stiffness behavior, modeled by the Duffing-Rayleigh equation, and a non-ideal motor that is connected to the end of the beam, is presented. Non-stationary and steady-state responses in the resonance region as well as the passage through resonance behavior when the frequency of the excitation is varied are analyzed. The influences of nonlinear stiffness, nonlinear damping and the extent of the unbalance in the motor are examined. It is found that in this situation so-called Sommerfeld effects may be observed; the increase required by a source operating near the resonance results in a small change in the frequency, but there is a large increase in the amplitude of the resultant vibration and the jump phenomenon occurs.

1. Introduction

When the excitation is not influenced by the response of a vibrating system, it is said to be an ideal system (traditional ones), or an ideal energy source. Formally, the excitation may be expressed as a pure function of time connected to a nonlinear oscillator whose dynamics of this system may be described by the equation

$$\ddot{x} + f_1(x, \dot{x}) + f_2(x) = F(t), \tag{1}$$

where x refers to the displacement of the primary system, f_1 represents the Van der Pol and Rayleigh function, f_2 represents the Duffing function and $F(t)$ is the harmonic external force. This nonlinear differential equation

*Corresponding author.
E-mail address: jmbaltha@rc.unesp.br (J.M. Balthazar).
[1]Permanent address: Department of Structural and Geotechnical Engineering Polytechnic School, University of Sao Paulo, Sao Paulo, Brazil.

0022-460X/$ - see front matter © 2008 Elsevier Ltd. All rights reserved.
doi:10.1016/j.jsv.2008.06.036

is used in physics, engineering, electronics and many other disciplines. The nonlinear mechanical oscillators have been studied extensively [1–3].

For non-ideal dynamical systems, the excitation of the vibration systems analyzed here is always limited: on the one hand by the characteristics of a particular energy source and on the other hand by the dependence of the motion of the oscillating system on the motion of the energy source. Formally, one must add an equation that describes how the energy source supplies the energy to the equations that govern the corresponding ideal dynamical system. In this case the non-ideal nonlinear system can be described by the following system of coupled differential equations:

$$\begin{aligned} &m\ddot{x} + f_1(x,\dot{x}) + f_2(x) = F(\varphi,\dot{\varphi},\ddot{\varphi},q),\\ &I\ddot{\varphi} + H(\dot{\varphi}) = L(\dot{\varphi}) + R(\varphi,\dot{\varphi},\ddot{x},q), \end{aligned} \tag{2}$$

where $F(\varphi,\dot{\varphi},\ddot{x},q)$ express the action of the source of energy on the oscillating system (angular velocity of the motor is not constant), q is the unbalanced coefficient (electric motor with eccentricity), I is the moment of inertia of mass, the function $R(\varphi,\dot{\varphi},\ddot{x},q)$ express the action of the oscillating system on the source of energy, the function $H(\dot{\varphi})$ is the resistive torque applied to the motor, the function $L(\dot{\varphi})$ is the driving torque of the source of energy (motor), the function $f_1 = (c_1 + c_2\dot{x}^2)\dot{x}$ is called Rayleigh's function and it describe a nonlinear damping of the system and the function $f_2 = k_1x + k_2x^3$ is called Duffing's function and it describe a nonlinear stiffness.

Note that, usually, the inductance is much smaller than the mechanical time constant of the system and in stationary regime we can take $L(\dot{\varphi})$ as (linear) $L(\dot{\varphi}) = a - b\dot{\varphi}$, where a is related to the voltage applied across the armature of the DC motor, that is, a possible control parameter of the problem and b is a constant for each model of the DC motor considered.

Two important manifestations can lead to the so-called Sommerfeld effect: first, in the region before resonance on the atypical frequency–response curve, we note that as the power supplied to the source increases, the RPM of the motor increases accordingly. However, this behavior does not continue indefinitely. That is, closer the motor speed moves toward the resonant frequency the more power is required to increase the motor speed. More formally, a large change in the power supplied to the motor results in a small change in the frequency, but a large increase in the amplitude of the resulting vibrations. Thus, near resonance it appears that additional power supplied to the motor only increases the amplitude of the response while having little effect on the RPM of the motor. Second, the jump phenomena is a nonlinear effect that appears when a portion of the right branch of the frequency–response curve becomes unstable or when this curve becomes multivalued. As the driving frequency approaches the natural frequency, the vibrating system can suddenly jump from one side of resonance to the other. That is, the system operating in a steady-state mode cannot realize certain frequencies near resonance. The jump appears on the frequency-response curve as a discontinuity, which indicates a region where steady-state conditions do not exist [4–12].

In this paper, by using the averaging method, we prove the presence of the Sommerfeld effect on a Duffing-Rayleigh oscillator with non-ideal excitation of periodic and quasi-periodic motion in the stationary and non-stationary regimes through resonance as an extension of Refs. [9,13,14]. Moreover, we determine the conditions to compute the maximum and jump points of the resonance curve. For the determination of the Lyapunov exponents the averaging system is also utilized.

We organize this paper as follows. In Section 2, we present the mathematical model used and the derivation of the governing equations of motion. In Section 3, we obtain an analytical solution to the analyzed problem, by using an average procedure to the non-ideal dynamics of the adopted oscillating problem. In Section 4, we analyzed the non-stationary solutions. In Section 5, we analyzed the steady-state solutions. In Section 6, we analyzed the special points of the steady-state solutions that define the maximum point and jump point in the response–frequency curve. In Section 7, we analyzed the influence of the parameters, which in this case are chosen as the coefficients of nonlinear stiffness and damping. In Section 8, we analyzed the dynamical behavior of the system with Lyapunov exponents on the non-stationary system. In Section 9, we analyzed the original system considering stiffness of the softening type where we observe a chaotic regime. In Section 10, we mention the concluding remarks of this work. Finally comes the acknowledgements and list of the main references used.

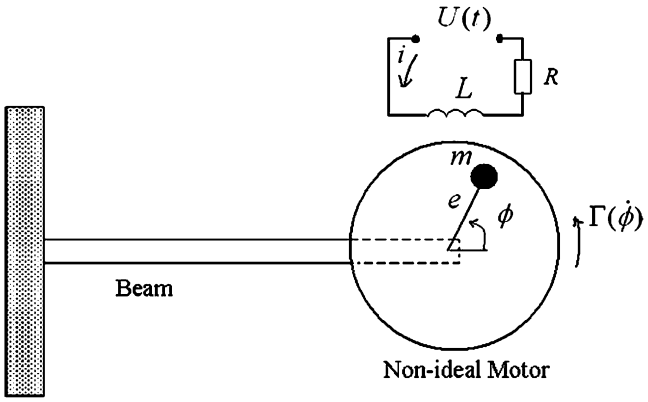

Fig. 1. Model of the non-ideal cantilever beam.

2. Model of the non-ideal nonlinear system

We consider the non-ideal problem consisting of a nonlinear cantilever beam supporting an unbalanced motor with limited power at its free end (see Fig. 1). Its representative mathematical formulation depend on the Lagrange formulation for a system that has two degrees of freedom, represented by the generalized coordinates x (cantilever beam displacement) and ϕ (angular displacement of the rotor unbalance). The kinetic energy T, potential energy V, the dissipative function of the beam G_B and the torque exerted by the motor $\Gamma(\dot{\phi})$ are expressed by

$$\begin{aligned} &T = \tfrac{1}{2}M\dot{x}^2 + \tfrac{1}{2}J\dot{\phi}^2 + \tfrac{1}{2}m(\dot{x} - \mathrm{e}\dot{\phi}\cos\phi)^2 + \tfrac{1}{2}m(\mathrm{e}\dot{\phi}\sin\phi)^2,\\ &V = \tfrac{1}{2}k_1x^2 + \tfrac{1}{2}k_2x^4,\\ &G_B = -\tfrac{1}{2}c_1\dot{x} - \tfrac{1}{2}c_2\dot{x}^3, \quad \Gamma(\dot{\phi}) = L(\dot{\phi}) - H(\dot{\phi}), \end{aligned} \tag{3}$$

where $L(\dot{\phi})$ (depending of the tension $U(i)$) is the driving torque and $H(\dot{\phi})$ is the resisting torque.

In this paper, we will extend the work of Bolla et al. [13], introducing the cubic nonlinear damping (the function G_B) and the reduced model, which exhibits on Warminski et al. [9] with parametric coefficient $\mu = 0$. We obtain a nonlinear differential equation of the Duffing-Rayleigh type driven by a non-ideal energy source in a dimensionless form:

$$\begin{aligned} &\ddot{X} + (-\alpha + \beta\dot{X}^2)\dot{X} + (1 + \gamma X^2)X = q_1(\ddot{\phi}\cos\phi - \dot{\phi}^2\sin\phi),\\ &\ddot{\phi} = \Gamma(\dot{\phi}) + q_2\ddot{X}\cos\phi. \end{aligned} \tag{4}$$

From this we adopt a dot as the differentiation with respect to dimensionless time τ and we assume that the motor's torque is a linear function of its angular velocity $\Gamma(\dot{\phi}) = V_m - C_m\dot{\phi}$, V_m is considered as a control parameter and it can be changed according to the voltage of the DC motor, C_m is a constant for each model of the DC motor considered, α is the coefficient of linear damping, β is the nonlinear damping coefficient, γ is the nonlinear stiffness coefficient, q_1 and q_2 are the unbalanced coefficients, the natural frequency is one unity, X is the coordinate oscillatory motion of the considered cantilever beam and $\dot{\phi}$ is the angular velocity of the motor.

3. Averaging equations

In this section, we use the method of averaging [4,15,16] to determine an approximate solution and average equations. To this end, Eq. (4) is rewritten as

$$\begin{aligned} &\ddot{X} + X = \varepsilon\{\hat{\alpha}\dot{X} - \hat{\beta}\dot{X}^3 - \hat{\gamma}X^3 + \hat{q}_1(\ddot{\phi}\cos\phi - \dot{\phi}^2\sin\phi)\},\\ &\ddot{\phi} = \varepsilon\{\hat{q}_2\ddot{X}\cos\phi + \hat{\Gamma}(\dot{\phi})\}, \end{aligned} \tag{5}$$

where

$$\alpha = \varepsilon\hat{\alpha},\ \ \beta = \varepsilon\hat{\beta},\ \ \gamma = \varepsilon\hat{\gamma},\ \ q_1 = \varepsilon\hat{q}_1,\ \ q_2 = \varepsilon\hat{q}_2,$$
$$\Gamma(\dot{\phi}) = V_m - C_m\dot{\phi} = \varepsilon\hat{\Gamma}(\dot{\phi}) \tag{6}$$

and ε, $0<\varepsilon<1$ is an arbitrary small parameter. We apply the method of variation of parameters and let

$$X = a\cos(\phi + \xi), \tag{7}$$

$$\dot{X} = -a\sin(\phi + \xi), \tag{8}$$

$$\dot{\phi} = \Omega, \tag{9}$$

where a, ξ and Ω are the new coordinates. In the regime near resonant, the difference between the excitation frequencies is close to the natural frequency:

$$\Omega = 1 + \varepsilon\sigma, \tag{10}$$

where σ is a detuning parameter.

The first derivative of Eq. (7)

$$\dot{X} = \dot{a}\cos(\phi + \xi) - a(\Omega + \dot{\xi})\sin(\phi + \xi). \tag{11}$$

It follows from Eqs. (8) and (11) that

$$\dot{a}\cos(\phi + \xi) - a\dot{\xi}\sin(\phi + \xi) = a(\Omega - 1)\sin(\phi + \xi). \tag{12}$$

Differentiating Eq. (8) gives

$$\ddot{X} = -\dot{a}\sin(\phi + \xi) - a(\Omega + \dot{\xi})\cos(\phi + \xi). \tag{13}$$

Substituting Eqs. (10), (11) and (13) into Eq. (5) gives

$$-\dot{a}\sin(\phi + \xi) - a\dot{\xi}\cos(\phi + \xi) = a(\Omega - 1)\cos(\phi + \xi) + \varepsilon f_1, \tag{14}$$

where

$$f_1 = -\hat{\alpha}a\sin(\phi + \xi) + \hat{\beta}a^3\sin^3(\phi + \xi) - \hat{\gamma}a^3\cos^3(\phi + \xi) + q_1\Omega^2\sin\phi. \tag{15}$$

Applying the trigonometric identities:

$$\sin^2\theta = \tfrac{1}{2} - \tfrac{1}{2}\cos 2\theta, \quad \sin^4\theta = \tfrac{1}{8}(\cos 4\theta - 4\cos 2\theta + 3),$$
$$\cos^4\theta = \tfrac{1}{8}(\cos 4\theta + 4\cos 2\theta + 3), \quad \sin^3\theta\cos\theta = \tfrac{1}{8}(2\sin 2\theta - \sin 4\theta),$$
$$\cos^3\theta\sin\theta = \tfrac{1}{8}(2\sin 2\theta + \sin 4\theta), \tag{16}$$

and considering the second equation of Eq. (5) in the resolution of the equations system for $\dot{a}$ and $\dot{\xi}$ from Eqs. (12) and (14), gives the following variational equations:

$$\dot{a} = -\varepsilon f_1\sin(\phi + \xi) = \varepsilon\Big(\tfrac{1}{2}\hat{\alpha}a - \tfrac{3}{8}\hat{\beta}a^3 + \tfrac{1}{2}\hat{q}_1\Omega^2\cos\xi + A_1(a, \xi, \phi, \Omega)\Big),$$

$$a\dot{\xi} = -\varepsilon a\sigma - \varepsilon f_1\cos(\phi + \xi) = \varepsilon\big(-a\sigma + \tfrac{3}{8}\hat{\gamma}a^3 - \tfrac{1}{2}\hat{q}_1\Omega^2\sin\xi + A_2(a, \xi, \phi, \Omega)\big),$$

$$\dot{\Omega} = \varepsilon(\hat{\Gamma}(\Omega) - \hat{q}_2 a\Omega\cos(\phi + \xi)\cos\xi + A_3(a, \xi, \phi, \Omega)), \tag{17}$$

where $A_1(a, \xi, \phi, \Omega)$, $A_1(a, \xi, \phi, \Omega)$ and $A_1(a, \xi, \phi, \Omega)$ are small periodic functions defined as follows:

$$A_1(a, \xi, \phi, \Omega) = \tfrac{1}{2}\hat{\alpha}a\cos(2\phi + 2\xi) + \tfrac{1}{8}\hat{\beta}a^3[\cos(4\phi + 4\xi) - 4\cos(2\phi + 2\xi)]$$
$$- \tfrac{1}{8}\hat{\gamma}a^3[2\sin(4\phi + 4\xi) + \sin(4\phi + 4\xi)] - \tfrac{1}{2}\hat{q}_1\Omega^2\cos(2\phi + \xi),$$

$$A_2(a,\xi,\phi,\Omega) = -\tfrac{1}{2}\hat{\alpha}a\sin(2\phi+2\xi)+\tfrac{1}{8}\hat{\beta}a^3[2\sin(2\phi+2\xi)-\sin(4\phi+4\xi)] -\tfrac{1}{8}\hat{\gamma}a^3[\cos(4\phi+4\xi)+4\cos(2\phi+2\xi)]+\tfrac{1}{2}\hat{q}_1\Omega^2\sin(2\phi+\xi),$$
$$A_3(a,\xi,\phi,\Omega) = -\tfrac{1}{2}\hat{q}_2 a\Omega\cos(2\phi+\xi). \quad (18)$$

We determine a first approximation from the average equations of the right-hand sides of Eq. (17) (considering a, ξ and Ω to be constants over one cycle and integrate (average) the equations over one cycle), and the result is

$$\dot{a} = \tfrac{1}{2}\alpha a - \tfrac{3}{8}\beta a^3 + \tfrac{1}{2}q_1\Omega^2\cos\xi,$$
$$\dot{\xi} = -(\Omega-1)+\tfrac{3}{8}\gamma a^2 - \tfrac{1}{2}q_1\frac{\Omega^2}{a}\sin\xi,$$
$$\dot{\Omega} = \Gamma(\Omega) - \tfrac{1}{2}aq_2\Omega\cos\xi, \quad (19)$$

where the first equation describes the variation of the amplitude of the oscillation (the behavior of the envelope of the oscillatory motion of the coordinate X), the second equation describes the variation of the initial phase of the motion ξ, the third equation describes the variation of the frequency Ω (the average value of the angular velocity of the motor). For the numerical simulation, the following values of parameters are considered: $\alpha = 0.1$, $\beta = 0.05$, $\gamma = 0.1$, $C_m = 1.5$, $q_1 = 0.2$ and $q_2 = 0.3$.

4. Non-stationary solutions

We first determine the amplitude, phase and average angular velocity of the response of Eq. (19) when $q_1 = q_2 = 0$ (there is no interaction between the structure support and the electric motor).

In this case, Eq. (19) can be written as

$$\dot{a} = \tfrac{1}{2}\alpha a - \tfrac{3}{8}\beta a^3,$$
$$\dot{\xi} = -(\Omega-1)+\tfrac{3}{8}\gamma a^2,$$
$$\dot{\Omega} = \Gamma(\Omega). \quad (20)$$

Solving the third equation of Eq. (20) yields:

$$\Omega = \frac{V_m}{C_m} + c_1\,\mathrm{e}^{-C_m\tau}, \quad c_1 = \Omega_0 - \frac{V_m}{C_m}. \quad (21)$$

Solving the first equation of Eq. (20) yields:

$$a = \frac{\sqrt{\alpha/2}\,\mathrm{e}^{\alpha(\tau+c_2)}}{(1+(3/8)\beta\,\mathrm{e}^{\alpha(\tau+c_2)})^{1/2}}, \quad c_2 = \frac{1}{\alpha}\ln\left(\frac{a_0}{(\alpha/2)-(3/8)\beta a_0^2}\right), \quad (22)$$

where a_0 and Ω_0 are the initial conditions.

We solve numerically Eq. (20) with initial conditions $a = 0.01$, $\xi = 0$, $\Omega = 0$ and $V_m = 1$ whose results are shown in Fig. 2 and then we validate Eqs. (21) and (22).

Considering $q_1 \neq 0$ and $q_2 \neq 0$ for the system in Eq. (19) with $q_1 = 0.2$ and $q_2 = 0.3$, the dynamical interaction between the cantilever beam and the electric motor is then active and manifestation of the Sommerfeld effect is present. The time response of the amplitude a and angular velocity Ω in the non-stationary regime are shown in Fig. 3 during the passage through resonance. In the time ranges $200 \leqslant \tau \leqslant 350$ and $600 \leqslant \tau \leqslant 1500$, there exists a synchronization of motion and oscillations between a and Ω; in this case the response of X is quasi-periodic motion. In the time range $350 < \tau < 600$ (resonance capture region) the amplitude and angular velocity are constant, then the vibration response of the system is of periodic motion.

For the control parameter range $0.5 \leqslant V_m \leqslant 1.4$, the response of X is of quasi-periodic motion, for example, for $V_m = 1.0$ is justified by a close curve shown on phase portrait (Fig. 4a). For the range $1.4 \leqslant V_m \leqslant 2.4$, the response of X is of periodic motion, in this case, for $V_m = 1.8$ is justified by one point shown on phase portrait (Fig. 4b). For the range $2.24 \leqslant V_m \leqslant 6.0$, the response of X is of quasi-periodic motion, in this case, for $V_m = 3.0$ is justified by a close curve shown on phase portrait (Fig. 4c).

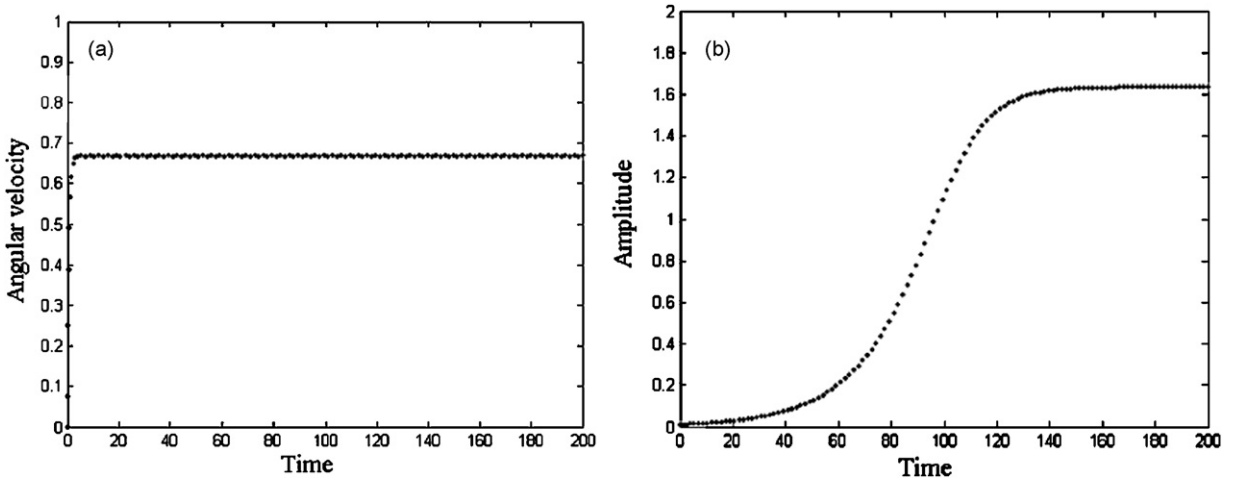

Fig. 2. Response as a function of the dimensionless time: (a) average angular velocity $\Omega(\tau)$ and (b) amplitude $a(\tau)$.

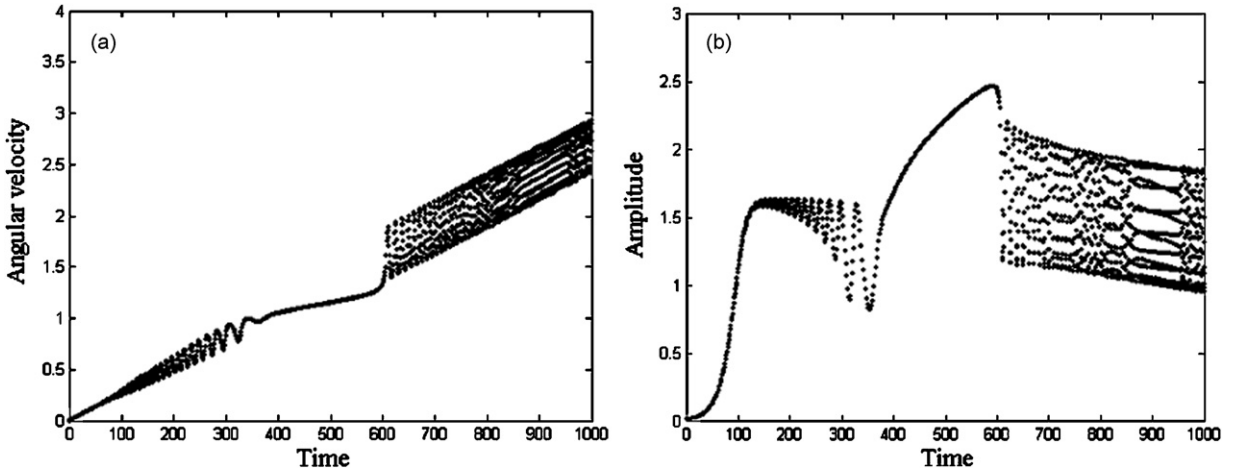

Fig. 3. Non-stationary response as a function of the dimensionless time: (a) angular velocity $\Omega(\tau)$ and (b) amplitude $a(\tau)$.

5. Steady-state solutions

The values of a, Ω and ξ for the stationary conditions of motion are determined as the roots of the system of equations:

$$\begin{aligned} &\tfrac{1}{2}\alpha a - \tfrac{3}{8}\beta a^3 + \tfrac{1}{2}q_1\Omega^2\cos\xi = 0,\\ &-(\Omega-1) + \tfrac{3}{8}\gamma a^2 - \tfrac{1}{2}q_1\frac{\Omega^2}{a}\sin\xi = 0,\\ &\Gamma(\Omega) - \tfrac{1}{2}aq_2\Omega\cos\xi = 0. \end{aligned} \tag{23}$$

Combining the first and second equations of Eq. (23) yields:

$$a^2\left[\left(\frac{3}{8}\beta a^2 - \frac{\alpha}{2}\right)^2 + \left((\Omega-1) - \frac{3}{8}\gamma a^2\right)^2\right] = \left(\frac{1}{2}q_1\Omega^2\right)^2. \tag{24}$$

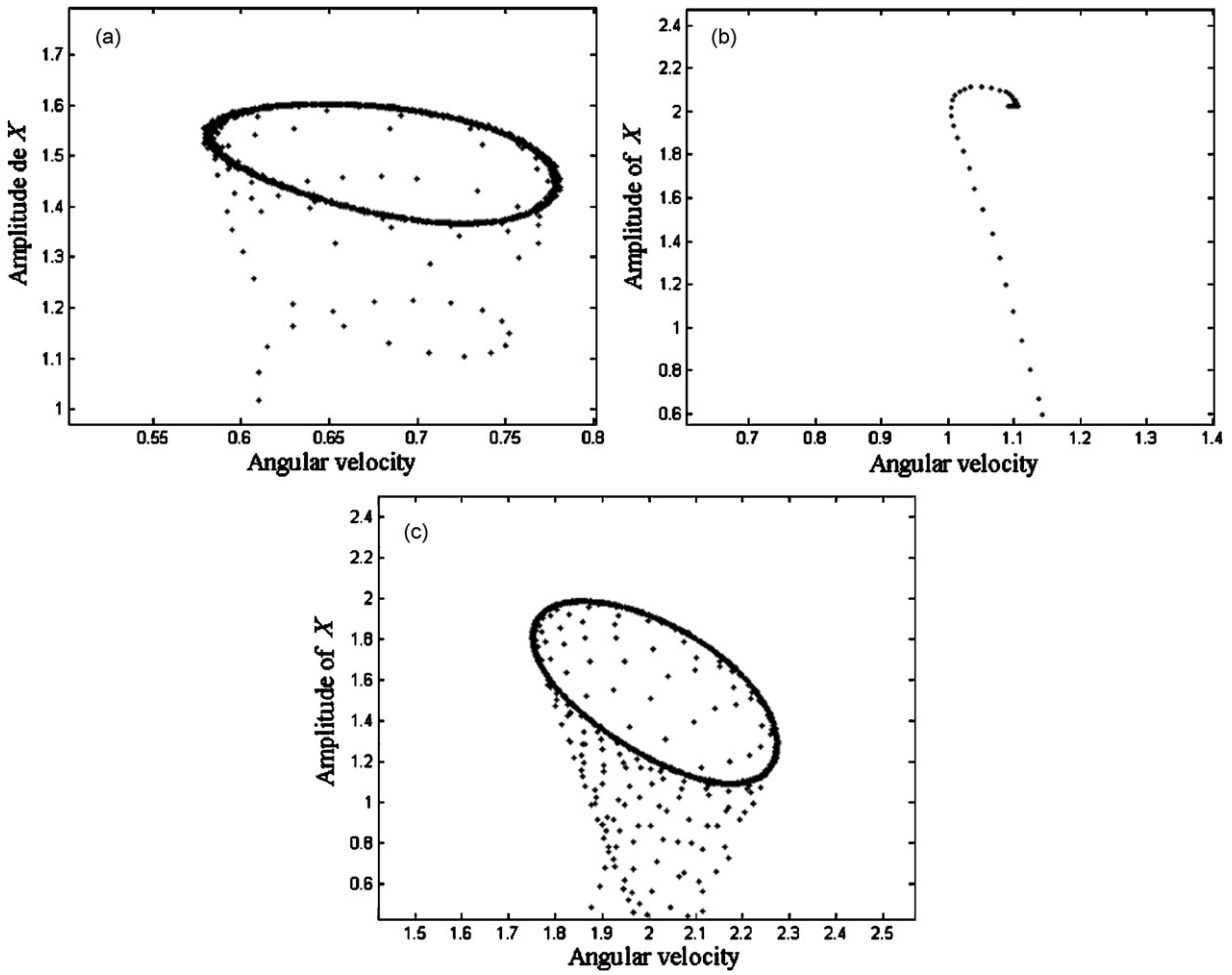

Fig. 4. Phase portrait in the plane $(\Omega(\tau), X(\tau))$ for (a) $V_m = 1.0$, (b) $V_m = 1.8$ and (c) $V_m = 3.0$.

Combining the first and third equations of Eq. (23) yields:

$$\frac{\alpha}{2}a^2 - \frac{3}{8}\beta a^4 + \frac{q_1}{q_2}\Omega\Gamma(\Omega) = 0. \tag{25}$$

The amplitude of the cantilever beam and the rotational frequency of motor are determined from Eqs. (24) and (25), respectively, for each value of the control parameter V_m. The phase of motion in the steady-state responses is given by

$$\tan\xi = \frac{(3/8)\gamma a^2 - \Omega + 1}{(3/8)\beta a^2 - (1/2)\alpha}. \tag{26}$$

The stability of an averaging solution is then determined by the eigenvalues of the Jacobian of the average system at the average solution. The Jacobian of the average equations is given by

$$J = \begin{bmatrix} \frac{\alpha}{2} - \frac{9}{8}\beta a^2 & -\frac{1}{2}q_1\Omega^2\sin(\xi) & q_1\Omega\cos(\xi) \\ \frac{6}{8}\gamma a + \frac{q_1}{8a^2}\Omega^2\sin(\xi) & -\frac{q_1}{2a}\Omega^2\cos(\xi) & -1 - \frac{q_1}{a}\Omega\sin(\xi) \\ -\frac{q_2}{2}\Omega\cos(\xi) & \frac{q_2 a\Omega}{2}\sin(\xi) & -C_m - \frac{q_2}{2}a\cos(\xi) \end{bmatrix}. \tag{27}$$

The characteristic equation of the Jacobian, evaluated at the average solution (Eqs. (24) and (25)), is then

$$J_3\lambda^3 + J_2\lambda^2 + J_1\lambda + J_0 = 0, \tag{28}$$

where

$$J_1 = \frac{1}{2}q_1\Omega^2\left(\frac{6\gamma a}{8} + \frac{q_1\Omega^2}{8a^2}\sin\,\xi\right)\sin\,\xi + \frac{q_1q_2\Omega^2}{2}\cos^2\xi - \frac{q_1\Omega^2}{2a}\left(\frac{\alpha}{2} - \frac{9\beta}{8}a^2\right)\cos\xi$$
$$- \left(C_m + \frac{q_2a}{2}\cos\xi\right)\left(\frac{\alpha}{2} - \frac{9\beta}{8}a^2\right) + \frac{q_1\Omega^2}{2a}\cos\xi\left(C_m + \frac{q_2a}{2}\cos\xi\right) + \left(1 + \frac{q_1\Omega}{a}\sin\xi\right)\frac{q_2\Omega a}{2}\sin\,\xi,$$

$$J_0 = -\det(J), \quad J_3 = 1, \quad J_2 = -\frac{\alpha}{2} + \frac{9\beta}{8}a^2 + \frac{q_1\Omega^2}{2a}\cos\xi + \frac{q_2a}{2}\cos\xi + c_m. \tag{29}$$

For stable averaging solutions, the eigenvalues of the Jacobian, or the roots of the above characteristic equation, must have negative real parts. According to the Routh-Hurwitz criterion, the real part of all eigenvalues is less than zero and if the following conditions are satisfied:

$$J_0 > 0 \Leftrightarrow \det(J) < 0, \quad J_1 > 0, \quad J_2 > 0, \quad J_2J_1 - J_0 > 0. \tag{30}$$

The criterion of the stationary solutions according to Nayfeh and Mook [4] is that the steady-state motion of an ideal system is determined by two forms.

Firstly, by direct integration of Eq. (19), then during a long time, the averaging approximates that a, Ω and ξ tend to constant values.

Secondly, the constant solution is obtained by setting the left-hand sides of Eq. (23) to zero ($\dot{a} = 0$, $\dot{\Omega} = 0$, $\dot{\xi} = 0$).

But in this case, for a non-ideal system it is different; for example, considering the values $V_m = 1.8$ the responses of Ω (left hand of Fig. 5) and a (right hand of Fig. 5) become constant motion in the time range $40 \leqslant \tau \leqslant 200$. When $V_m = 3.0$, the responses of Ω (left hand of Fig. 6) and a (right hand of Fig. 6) become oscillating motion in a long time. In this case, we cannot determine a solution directly using the Newton method to the non-ideal problem in the solution of the system of Eq. (23).

Fig. 7 shows the resonance curve of vibration amplitudes of the beam and angular velocity of the motor versus the sequence increase of the control parameter on steady-state motion. For the ranges $0.6 \leqslant V_m \leqslant 1.31V_m$ and $2.24 \leqslant \mathrm{V}_m \leqslant 7.0$, one may observe that the responses of the amplitude (left hand of Fig. 7) and angular velocity (right hand of Fig. 7) are oscillating (marked by two dots, denoting the oscillating extremes), then we generate the quasi-periodic motion in the non-ideal system, which is obtained by strong interaction between the beam and the motor [9]. For the range $1.32 \leqslant V_m \leqslant 2.23$, the response of the amplitude and angular velocity is constant (marked by a dot); then we generate periodic motion in the non-ideal system.

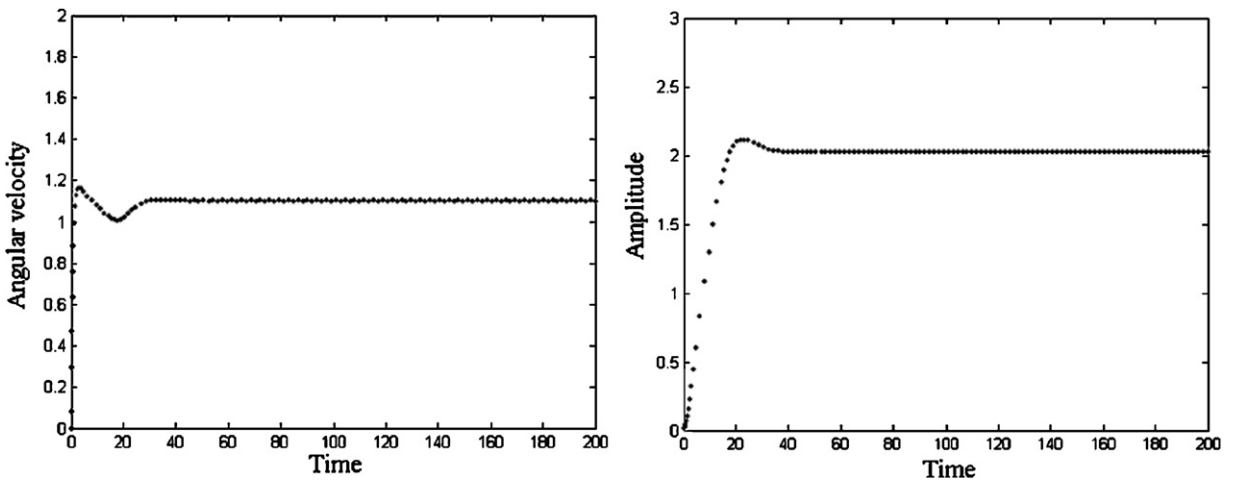

Fig. 5. Response of the angular velocity $\Omega(\tau)$ and amplitude $a(\tau)$ for $V_m = 1.8$.

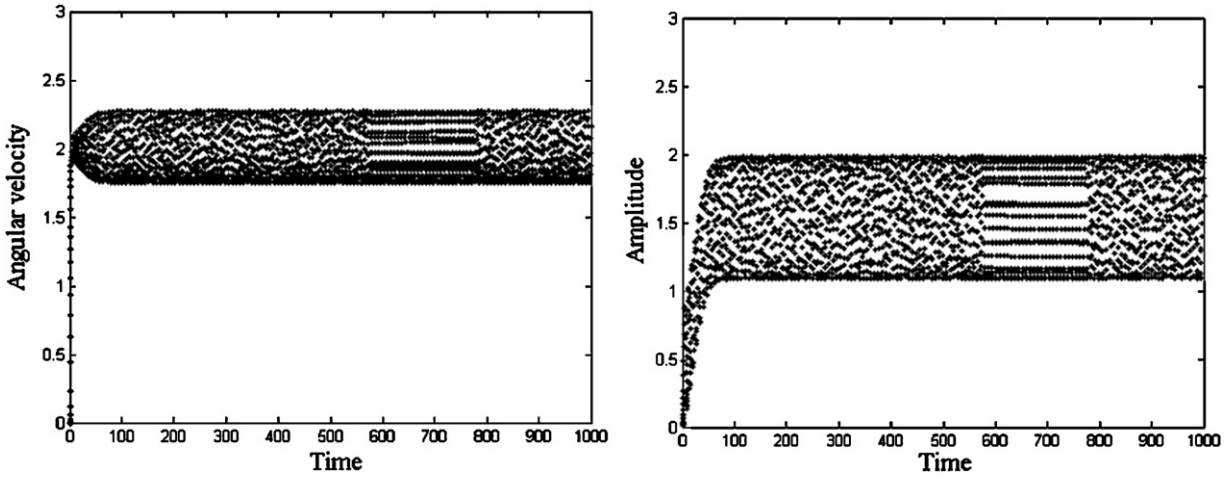

Fig. 6. Response of the angular velocity $\Omega(\tau)$ and amplitude $a(\tau)$ for $V_m = 3.0$.

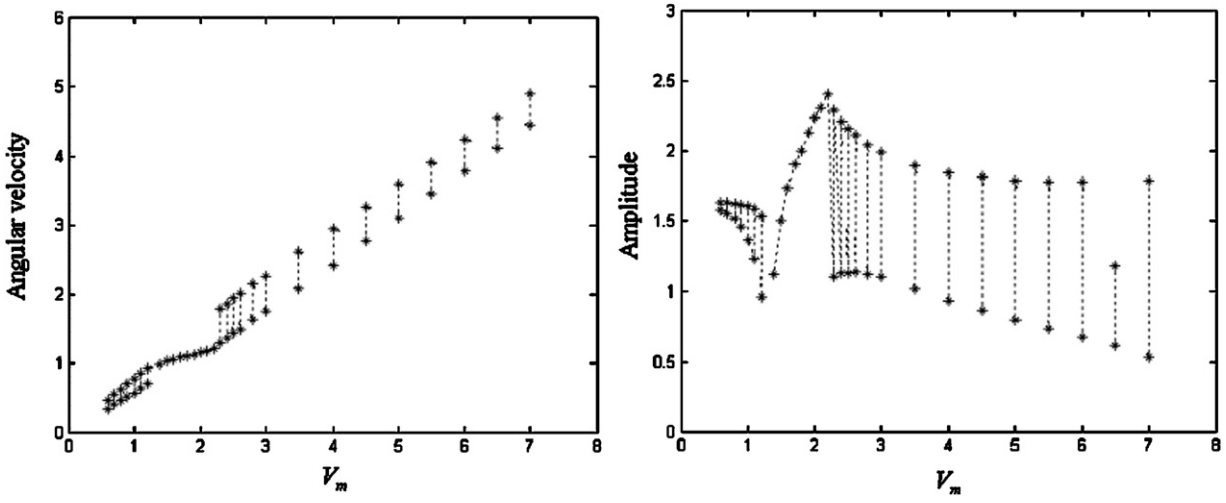

Fig. 7. Curves of responses versus control parameter in steady-state process of $\Omega(\tau)$ and $a(\tau)$ in the range $0.6 \leqslant V_m \leqslant 7.0$.

6. Special points

In this section, we analyze the special points of the steady-state solutions that define the maximum point and jump point in the response–frequency curve.

We define $\Omega - 1 = \Delta\Omega$ in the approximating of jump and we write Eq. (24) as

$$a^2\left[\left(\frac{3}{8}\beta a^2 - \frac{\alpha}{2}\right)^2 + \left(\Delta\Omega - \frac{3}{8}\gamma a^2\right)^2\right] = \left(\frac{1}{2}q_1\Omega^2\right)^2. \tag{31}$$

From this we can determine the locus of the peak corresponding to rotational frequency in the frequency–response curve. Making $\Delta\Omega - (3/8)\gamma a^2 = 0$, we obtain

$$\Omega_p = 1 + \tfrac{3}{8}\gamma a_p^2, \tag{32}$$

and the peak of the amplitude is determined as the roots of the following equation:

$$a_p\left(\frac{3}{8}\beta a_p^2-\frac{\alpha}{2}\right)-\frac{1}{2}q_1\Omega_p^2=0. \tag{33}$$

Then, the control parameter corresponding to this peak of jump, from Eq. (25), is given by

$$V_{\mathrm{mp}}=\frac{(3/8)\beta q_2 a_p^4-(\alpha q2/2)a_p^2+q_1C_m\Omega_p^2}{q_1\Omega_p}. \tag{34}$$

Thus, with this control parameter value we can eliminate the Sommerfeld effect. To determine the maximum points, we write Eq. (25) in the following form:

$$\frac{\alpha q_2}{2}a^2-\frac{3q_2\beta}{8}a^4+q_1\Delta\Omega(V_m-C_m\Delta\Omega)=0. \tag{35}$$

Differentiating Eq. (35) with respect to $\Delta\Omega$ and demanding $\mathrm{d}(a)/\mathrm{d}\Delta\Omega=0$ yields $\Delta\Omega=(V_m/2C_m)$, then the critical frequency of maximum is

$$\Omega_c=1+\frac{V_m}{2C_m} \tag{36}$$

and the critical amplitude of maximum, using Eqs. (25) and (36), is determined by

$$a_c^4-\frac{4\alpha}{3\beta}a_c^2-\frac{4q_1V_m}{3\beta q_2C_m}\left(\frac{V_m}{2}-C_m\right)=0. \tag{37}$$

7. Influence of the parameters in a non-stationary system

In this section, we observe the influence of the parameters of nonlinearities that are the coefficients of nonlinear stiffness and damping (γ,β). The numerical results of the system from Eq. (19) are presented in time history where the left diagram corresponds to the response of the angular velocity of the motor and the right diagram corresponds to the response of the amplitude of the cantilever beam on the control parameter range $0.6\leqslant V_m\leqslant 7.0$, while the other parameters are fixed (see Figs. 8 and 9).

Firstly, we present the effect of the nonlinear stiffness. Fig. 8 illustrates the behavior of two non-stationary responses that is the comparison for two values of nonlinear stiffness taken as $\gamma=0.05$ and $\gamma=0.2$. The jump

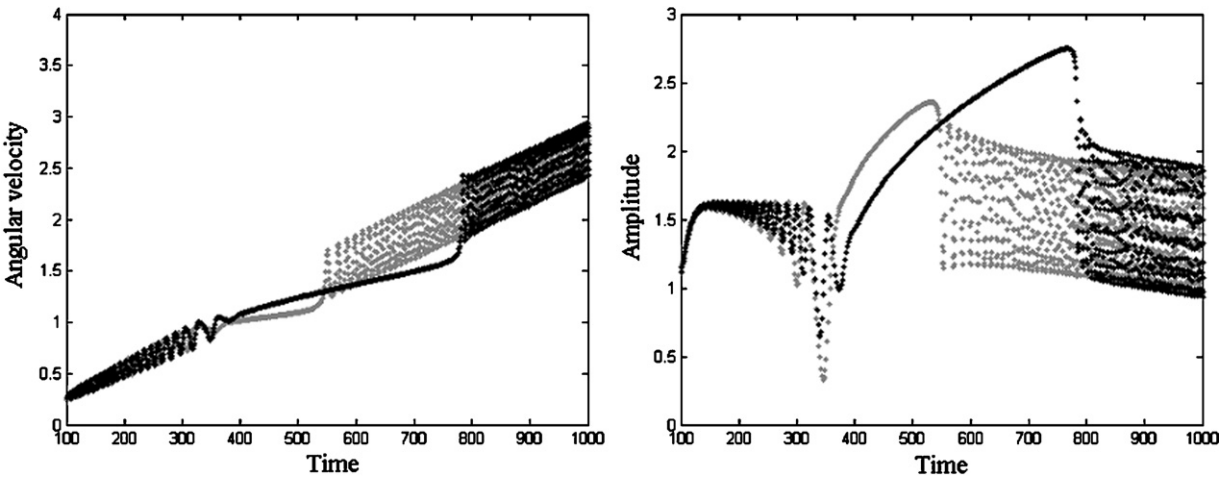

Fig. 8. Effect of the nonlinear stiffness on time response in the non-stationary process of $\Omega(\tau)$ and $a(\tau)$ for $\gamma=0.05$ (gray line) and $\gamma=0.2$ (black line).

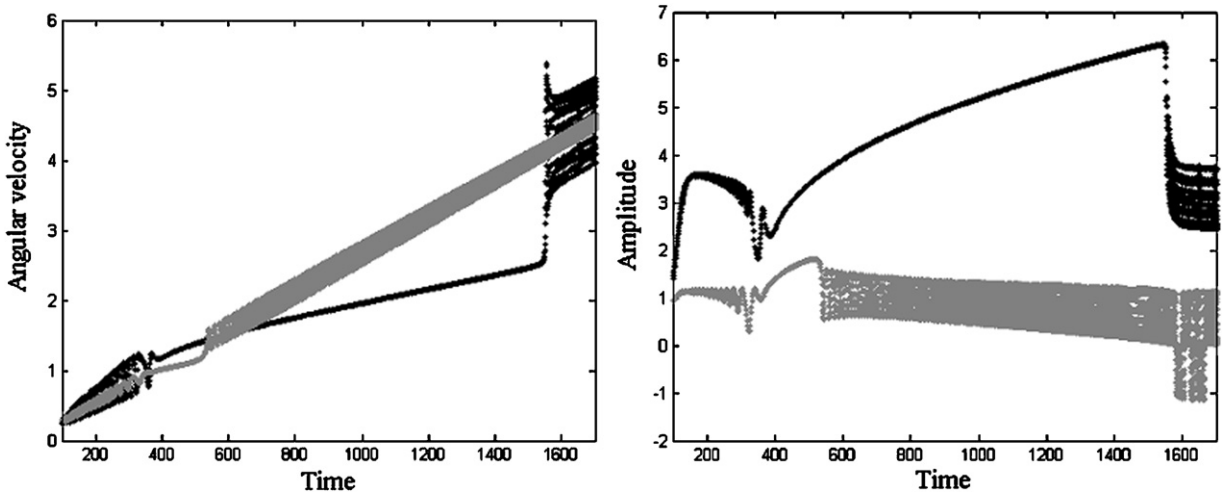

Fig. 9. Effect of nonlinear damping on time response in the non-stationary process of $\Omega(\tau)$ and $a(\tau)$ for $\beta = 0.01$ (black line) and $\beta = 0.1$ (gray line).

Table 1
Lyapunov's exponents

V_m	Attractor's type	λ_1	λ_2	λ_3
1.0	Quasi-periodic	0.0	−0.079135	−0.145964
1.8	Periodic	−0.2192	−0.227961	−1.401873
3.0	Quasi-periodic	0.0	−0.089585	−1.544268

phenomenon happens for $\gamma = 0.05$ and $\gamma = 0.2$ in the time ranges $500 < \tau < 600$ and $750 < \tau < 850$, respectively. Then to eliminate the jump phenomenon or the effect of Sommerfeld, we need to consider $\gamma < 1$. But we observe that the motor of limited power is not captured or stagnated in the resonance region for $\gamma = 0.2$ while the oscillation amplitude of the beam is increasing. Secondly, we present the effect of nonlinear damping. Fig. 9 illustrates the behavior of two non-stationary responses, that is the comparison for two values of nonlinear damping $\beta = 0.01$ and $\beta = 0.1$. The jump phenomenon is present in different zones passing through the resonance region. Then to eliminate the jump phenomenon or Sommerfeld effect, it is necessary to increase the value of the nonlinear damping. In this case, the resonance capture of the angular velocity and the vibration amplitude of the foundation are reduced.

8. Lyapunov exponents of the averaging system

In order to complete the dynamic analysis, we evaluate the Lyapunov exponents, using the classical method described in Ref. [17]. The main expression is

$$\lambda = \frac{1}{tN}\sum_{i=1}^{N} \ln\left(\frac{d_i(t)}{d_i(0)}\right), \tag{38}$$

where λ denotes the Lyapunov exponents, the index i represents consecutive initial positions, N represents the total step number of evolution and d is the separation between two close trajectories, chosen. We remarked that Eqs. (19) and (27) are conditioned in the MATDS® program [18], based on the routine of Matlab® of Matworks®, in order to evaluate Lyapunov's exponents, which are listed in Table 1. Note that if we take into account $V_m = 1.0$ and $V_m = 3.0$, we obtain the confirmation that the considered non-ideal system vibrates in

quasi-periodical motion (one Lyapunov exponent is zero and the others are negative), and in the case where we take $V_m = 1.8$, one confirms that the non-ideal system vibrates periodically (the Lyapunov exponents are only negative).

9. Dynamics of the original system

In this section, to obtain a chaotic regime, we need to assume that the natural frequency is of negative value -1. It means that the linear term of the spring stiffness is softening [19]. Here, we consider the parameter $\gamma = 3.0$. To numerically solve the governing system of Eq. (5), the RK45 order numerical integration routine is selected with adaptive step size control according to Dormand and Prince [20]. Figs. 10a, 11a and 12a illustrate the diagrams of the phase portrait and Figs. 10b, 11b and 12b the power spectrum of the non-ideal system (beam response). Figs. 10 and 12 show that there is a periodic regime for $V_m = 3.0$ and $V_m = 6.0$, respectively (in cases both attractors of the system are limit cycles and the power spectrum is of one peak). Fig. 11 shows

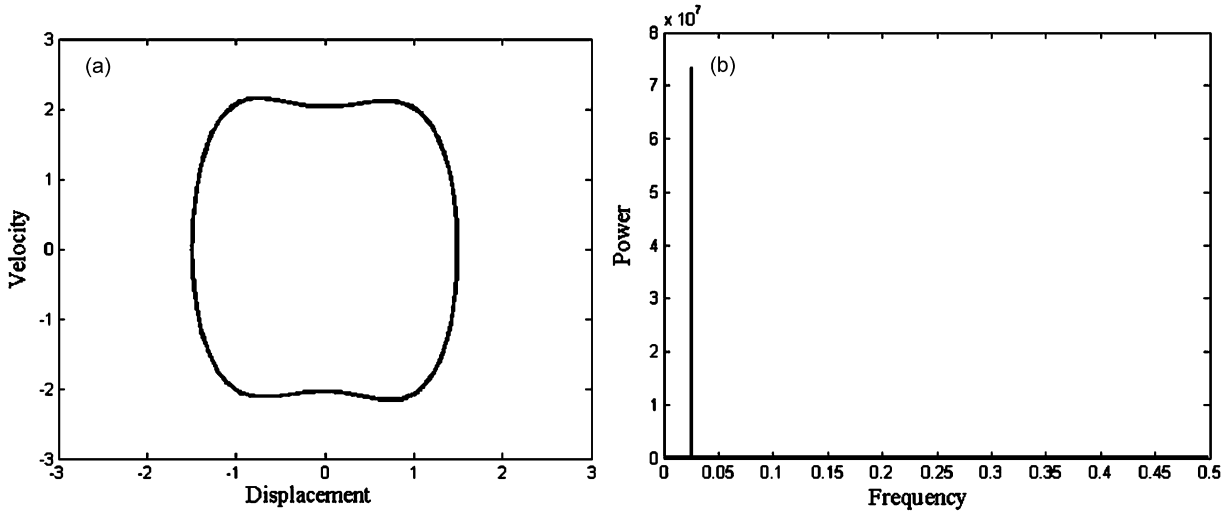

Fig. 10. Dynamic response of the beam for $V_m = 3.0$. (a) Phase portrait and (b) power spectrum.

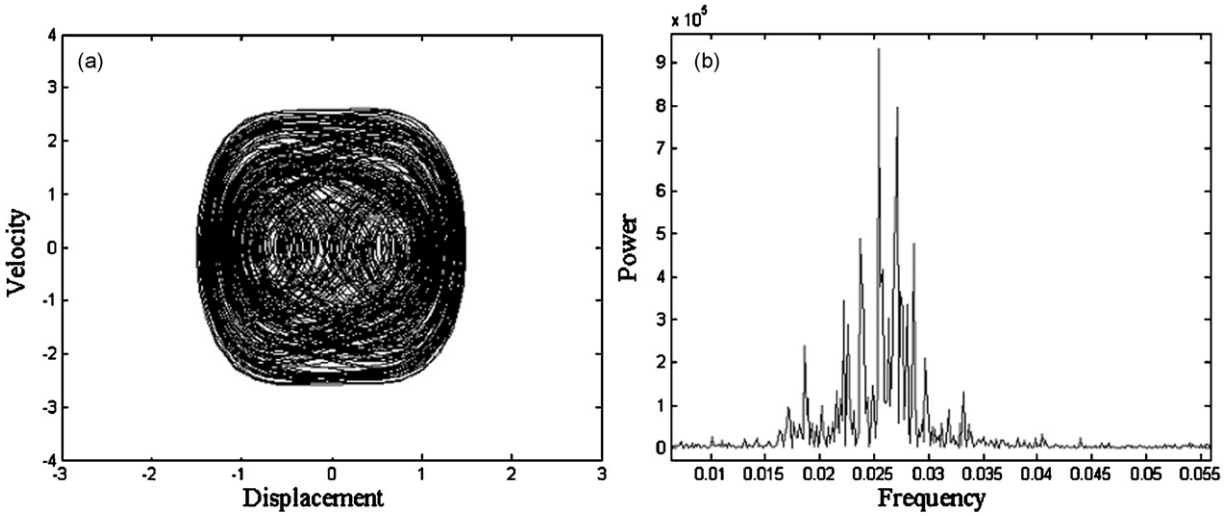

Fig. 11. Dynamic response of the beam for $V_m = 4.0$. (a) Phase portrait and (b) power spectrum.

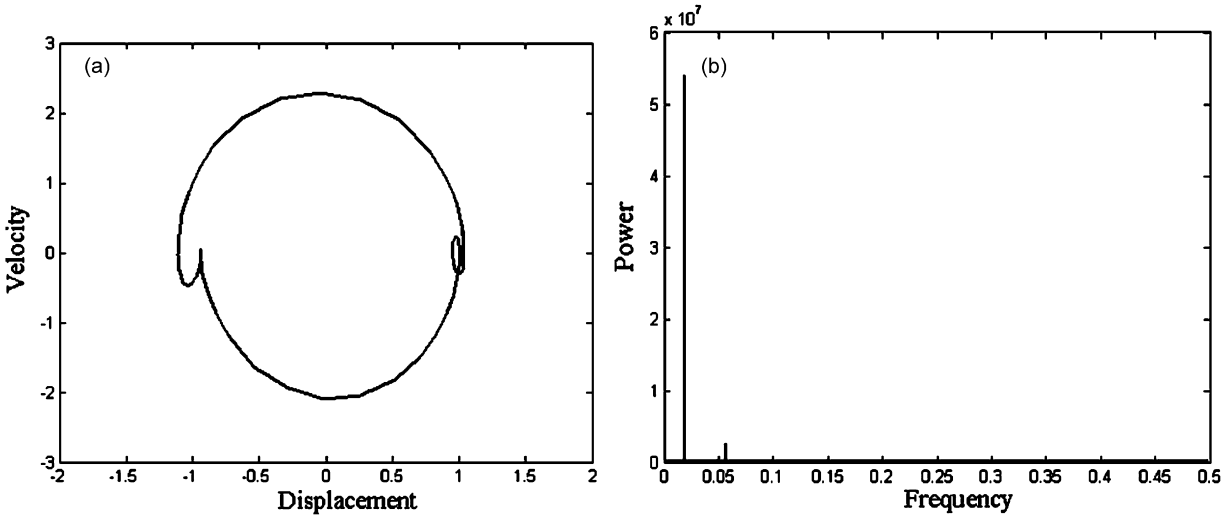

Fig. 12. Dynamic response of the beam for $V_m = 6.0$. (a) Phase portrait and (b) power spectrum.

that the non-ideal system is in chaotic regime for $V_m = 4.0$ (the attractor has divergence of the close phase trajectories and the power spectrum has a continuous structure and is characterized by the absence of peaks).

10. Conclusion

In this paper, we have demonstrated conclusively that nonlinear stiffness and damping in a cantilever beam oscillator, subject to a non-ideal excitation (unbalanced motor with limited power supply), may play an important role.

This fact makes this problem more realistic, according to the experimental results. The method of averaging discussed here may allow a systematic study of a non-ideal nonlinear system, which may help reveal the underlying physical mechanisms.

The Sommerfeld effect is reduced or eliminated when the value of the nonlinear stiffness is smaller than one (1) and the value of the nonlinear damping is increasing during the passage through the resonance region to the non-stationary and steady-state process.

We determinate the conditions of the special points for reducing or eliminating the manifestations of the Sommerfeld effect.

In the resonance region of the considered oscillation it has periodic motion and outside the resonance region it has quasi-periodic motion.

Acknowledgments

The first author acknowledges financial support by FAPESP (Fundação de Amparo à Pesquisa do Estado de São Paulo), under grant no 06/59742-2. The second and third authors acknowledge the support given by FAPESP and CNPq (Conselho Nacional de Desenvolvimento Científico).

References

[1] F.M. Kakmeni, S. Bowong, C. Tchawoua, E. Kaptouom, Strange attractors and control in a Duffing-van der Pol oscillator with two external periodic forces, *Journal of Sound and Vibration* 277 (2004) 783–799.

[2] J.P. Dada, J.C. Chedjou, S. Domngang, K. Kyamakya, Analytical, numerical and experimental analysis of a self-excited oscillator, *Physica Scripta* 74 (2006) 618–628.

[3] B. Ravindra, A.K. Mallik, Stability analysis of a non-linearly damped Duffing oscillator, *Journal of Sound and Vibration* 171 (5) (1994) 708–716.

[4] A.H. Nayfeh, D.T. Mook, *Nonlinear Oscillations*, Wiley, New York, 1979.
[5] J.M. Balthazar, D.T. Mook, H.I. Weber, R.M.L.R.F. Brasil, A. Fenili, D. Belato, J.L.P. Felix, An overview on non-ideal vibrations, *Meccanica* 38 (6) (2003) 613–621.
[6] V.O. Kononenko, *Vibrating Systems With Limited Power Supply*, Illife Books, London, 1969.
[7] M.J.H. Dantas, J.M. Balthazar, A comment on a non-ideal centrifugal vibrator machine behavior with soft and hard springs, *International Journal of Bifurcation and Chaos* 16 (4) (2006) 1083–1088.
[8] M.J.H. Dantas, J.M. Balthazar, On the existence and stability of periodic orbits in non-ideal problems: general results, *ZAMM Journal of Applied Mathematics and Mechanics* 940–956 (2007).
[9] J. Warminski, J.M. Balthazar, R.M.L.R.F. Brasil, Vibrations of a non-ideal parametrically and self-excited model, *Journal of Sound and Vibration* 245 (2) (2001) 363–374.
[10] M. Tsuchida, K.L. Guilherme, J.M. Balthazar, On chaotic vibrations of a non-ideal system with two degrees of freedom: 1:2 resonance and Sommerfeld effect, *Journal of Sound and Vibration* 282 (2005) 1201–1207.
[11] J.M. Balthazar, B.I. Chesankov, D.T. Ruschev, L. Barbanti, H.I. Weber, Remarks on the passage through resonance of a vibrating system with two degrees of freedom, excited by a non-ideal energy source, *Journal of Sound and Vibration* 239 (5) (2001) 1075–1085.
[12] A. Fenili, J.M. Balthazar, Some remarks on nonlinear vibrations of ideal and non-ideal slewing flexible structures, *Journal of Sound and Vibration* 282 (2005) 543–552.
[13] M.R. Bolla, J.M. Balthazar, J.L.P. Felix, On an approximate analytical solution to a nonlinear vibrating problem, excited by a non-ideal motor, *Nonlinear Dynamics* 50 (2007) 841–847.
[14] M. Zukovic, L. Cveticanin, Chaotic responses in a stable Duffing system on non-ideal type, *Journal of Vibration and Control* 13 (6) (2007) 751–767.
[15] A.H. Nayfeh, *Introduction to Perturbation Techniques*, Wiley, New York, 1981.
[16] J.L. Palacios, J.M. Balthazar, R.M.L.R.F. Brasil, On non-ideal and non-linear portal frame dynamics analysis using Bogoliubov averaging method, *Journal of the Brazilian Society Mechanical Sciences* 24 (4) (2005) 257–265.
[17] A. Wolf, J.B. Swift, H.L. Swinney, J.A. Vastano, Determining Lyapunov exponents from a time series, *Physica D* 16 (1985) 285–315.
[18] V.N. Govorukhin, MATDS—MATLAB-based for Dynamical System, 〈http://kvm.math.rsu.ru/matds〉, 2003.
[19] J. Warminski, Regular, chaotic and hyperchaotic vibrations of nonlinear systems with self, parametric and external excitations, *Series: Mechanics, Automatic Control and Robotics* 3 (14) (2003) 891–905.
[20] J.R. Dormand, P.J. Prince, A family of embedded Runge-Kutta formulae, *Journal of Computational and Applied Mathematics* 6 (1) (1980) 19–26.